

Published in final edited form as:

Biochemistry. 2011 March 15; 50(10): 1672–1681. doi:10.1021/bi101881d.

***Escherichia coli* class Ib ribonucleotide reductase contains a dimanganese(III)-tyrosyl radical cofactor in vivo†**

Joseph A. Cotruvo Jr[‡] and JoAnne Stubbe^{*,‡,§}

[‡] Department of Chemistry, Massachusetts Institute of Technology, Cambridge, MA 02139

[§] Department of Biology, Massachusetts Institute of Technology, Cambridge, MA 02139

Abstract

Escherichia coli class Ib ribonucleotide reductase (RNR) converts nucleoside 5'-diphosphates to deoxynucleoside 5'-diphosphates in iron-limited and oxidative stress conditions. We have recently demonstrated in vitro that this RNR is active with both diferric-tyrosyl radical ($\text{Fe}^{\text{III}}_2\text{-Y}\cdot$) and dimanganese(III)- $\text{Y}\cdot$ ($\text{Mn}^{\text{III}}_2\text{-Y}\cdot$) cofactors in the β_2 subunit, NrdF [Cotruvo J.A., Jr. and Stubbe J., *Biochemistry* (2010) 49, 1297–1309]. Here we demonstrate, by purification of this protein from its endogenous levels in an *E. coli* strain deficient in its five known iron uptake pathways and grown under iron-limited conditions, that the $\text{Mn}^{\text{III}}_2\text{-Y}\cdot$ cofactor is assembled in vivo. This is the first definitive determination of the active cofactor of a class Ib RNR purified from its native organism without overexpression. From 88 g of cell paste, 150 μg of NrdF was isolated with ~95% purity, with 0.2 $\text{Y}\cdot/\beta_2$, 0.9 Mn/β_2 , and a specific activity of 720 nmol/min/mg. In these conditions, the class Ib RNR is the primary active RNR in the cell. Our results strongly suggest that *E. coli* NrdF is an obligate manganese protein in vivo and that the $\text{Mn}^{\text{III}}_2\text{-Y}\cdot$ cofactor assembly pathway we have identified in vitro involving the flavodoxin-like protein NrdI, present inside the cell at catalytic levels, is operative in vivo.

Ribonucleotide reductases (RNRs)¹ catalyze the conversion of nucleotides to the deoxynucleotide building blocks required for DNA replication and repair (1). Class I RNRs are composed of two subunits: α_2 , where nucleotide reduction occurs, and β_2 , which contains the metallocofactor required for initiation of nucleotide reduction. *Escherichia coli* encodes two class I RNRs. Its class Ia RNR, NrdA (α_2) and NrdB (β_2), supplies and controls deoxynucleotide pools under normal aerobic growth conditions. Enzyme activity requires a diferric-tyrosyl radical ($\text{Fe}^{\text{III}}_2\text{-Y}\cdot$) cofactor in NrdB. Expression of the *E. coli* class Ib RNR, NrdE (α_2) and NrdF (β_2), is triggered under iron-limited and oxidative stress conditions (2–5), but its physiological role is unclear. By contrast, class Ib RNRs are the primary sources of dNTPs in aerobic growth for many prokaryotes, such as the human pathogens *Mycobacterium tuberculosis*, *Staphylococcus aureus*, *Bacillus anthracis*, and

[†]This research was supported by National Institutes of Health grant GM81393 to J.S. and a National Defense Science and Engineering Graduate (NDSEG) Fellowship to J.A.C.

^{*}To whom correspondence should be addressed. Tel: (617) 253-1814. Fax: (617) 324-0505. stubbe@mit.edu.

SUPPORTING INFORMATION AVAILABLE

Additional experimental details and results: assays of NrdB with NrdE and NrdF with NrdA, demonstration that NrdI does not activate $\text{Mn}^{\text{III}}_2\text{-NrdB}$, elution profile of the first FPLC step, and SDS-PAGE of partially purified NrdF. This material is available free of charge via the Internet at <http://pubs.acs.org>.

¹Abbreviations: α_2 , ribonucleotide reductase large subunit; β_2 , ribonucleotide reductase small subunit; bipy, 2,2'-dipyridyl; CDP, cytidine 5'-diphosphate; CV, column volume; dATP, deoxyadenosine 5'-triphosphate; EPR, electron paramagnetic resonance; FPLC, fast protein liquid chromatography; Ni-NTA, nickel nitrilotriacetic acid; PMSF, phenylmethanesulfonyl fluoride; RNR, ribonucleotide reductase; SDS-PAGE, sodium dodecyl sulfate–polyacrylamide gel electrophoresis; SPI2, *Salmonella* pathogenicity island 2; TR, thioredoxin; TRR, thioredoxin reductase; $\text{Y}\cdot$, tyrosyl radical

Streptococcus pyogenes (6). The identity of the metallocofactor required for activity of the class Ib RNRs in vivo has been debated for nearly three decades [summarized in (7)]. Although the class Ib RNR is active in vitro with a diferric-Y• cofactor (8), we recently characterized a dimanganese(III)-Y• ($\text{Mn}^{\text{III}}_2\text{-Y}\bullet$) cofactor in NrdF that is also active in nucleotide reduction (7). Here we demonstrate that the *E. coli* class Ib RNR uses this $\text{Mn}^{\text{III}}_2\text{-Y}\bullet$ cofactor inside the cell under defined, iron-limited growth conditions.

Only recently has evidence accumulated that class Ib RNRs very likely contain dimanganese cofactors inside the cell. Our in vitro experiments demonstrated for the first time that NrdF is competent to form a $\text{Mn}^{\text{III}}_2\text{-Y}\bullet$ cofactor active in nucleotide reduction, with a specific activity (600 nmol/min/mg for 0.25 Y•/β2) 4-fold higher on a per-Y• basis than that of the diferric-Y• cofactor (7). This $\text{Mn}^{\text{III}}_2\text{-Y}\bullet$ cofactor can be generated only by incubation of the dimanganese(II) form of the protein, $\text{Mn}^{\text{II}}_2\text{-NrdF}$, with the reduced form of a flavodoxin-like protein, NrdI, and O_2 . NrdI is universally conserved in class Ib systems, with the *nrdI* gene often found within the same operon as *nrdE* and *nrdF*. We proposed that the $\text{Mn}^{\text{III}}_2\text{-Y}\bullet$ cofactor is formed by reaction of $\text{Mn}^{\text{II}}_2\text{-NrdF}$ with two equivalents of H_2O_2 or HO_2^- [$\text{HOO}(\text{H})$], produced by two-electron reduction of O_2 by the reduced flavin cofactor of NrdI and channeled to the metal site. Support for this general mechanism has been recently provided by crystallization of the complex of $\text{Mn}^{\text{II}}_2\text{-NrdF}$ and NrdI (9), which revealed a channel between the two proteins through which the oxidant could be delivered. The biochemical and structural data led us to propose that the $\text{Mn}^{\text{III}}_2\text{-Y}\bullet$ cofactor is the active form of the *E. coli* class Ib RNR in vivo.

Recent work by Auling, Lubitz, and coworkers has demonstrated the ability of *Corynebacterium ammoniagenes* NrdF to form the same cofactor inside the cell (10,11). This NrdF was overexpressed in *C. ammoniagenes* to 5% of total cellular protein in the presence of 185 μM MnCl_2 in the growth media. The yield of purified NrdF was ~4 mg/g cells, with 0.36 Y•/β2, 1.5 Mn/β2, and a stated specific activity of 69000 nmol/min/mg. The EPR spectrum of the protein was identical to that of *E. coli* $\text{Mn}^{\text{III}}_2\text{-Y}\bullet$ NrdF reconstituted in vitro, and their extensive EPR analysis established that the cofactor is a ferromagnetically exchange-coupled Mn^{III}_2 cluster weakly coupled to a Y•.

The activity of both diiron and dimanganese forms of NrdF in vitro raises the question of how correct metallation is controlled in vivo (12,13). Overexpression of metalloproteins, even in their native organisms, can lead to mismetallation, but attempts to date to purify NrdFs after expression at their normal levels in several organisms have failed to yield sufficient active cofactor to allow its identification and biophysical characterization (14–16). We have therefore undertaken the purification of NrdF from its endogenous levels in *E. coli* under conditions in which transcriptional experiments (2–4,17) have suggested that NrdEF is maximally produced, namely iron limitation. Rensing and coworkers have created the *E. coli* strain GR536, which is deficient in the five known iron uptake pathways but is still able to import iron by one or more unknown pathway (18). They demonstrated that, after preculturing the strain in minimal media without added metals and dilution into minimal media containing the cell-permeable Fe^{II} chelator 2,2'-dipyridyl (bipy), growth is severely attenuated, but it is fully restored by addition of Mn^{II} (18). We hypothesized that Mn^{II} was limiting in these growth conditions, at least in part, because of an essential role in the class Ib RNR metallocofactor.

Here we present the purification of NrdF from this strain, the first purification of a NrdF without overexpression that allows for definitive determination of its active metallocofactor. *E. coli* GR536 cells were grown in Fe limitation in the presence of Mn^{II} and harvested in mid-exponential phase. From 88 g of cell paste, 150 μg NrdF with 0.20 Y•/β2, a specific activity of 720 nmol/min/mg, and 0.9 Mn/β2 was obtained. Spectroscopic and biochemical

data show that a $Mn^{III}_2\text{-Y}\cdot$ cofactor, not a $Fe^{III}_2\text{-Y}\cdot$ cofactor, is the active form of NrdF in *E. coli* under these growth conditions. Activity assays in crude extracts and western blotting analyses suggest that the class Ib RNR is the primary source of deoxynucleotides for *E. coli* in these growth conditions. Quantitative western blots also demonstrate that levels of NrdI are 13-fold lower than of NrdF, suggesting that NrdI acts catalytically in vivo in $Mn^{III}_2\text{-Y}\cdot$ generation. We suggest that *E. coli* NrdF is an obligate manganese protein. Furthermore, we propose that emerging data illustrating the requirement of pathogens such as *Salmonella enterica* serovar Typhimurium (*S. Typhimurium*), *S. aureus*, and *S. pyogenes* – all of which contain class Ib RNRs – for manganese for growth and virulence (19,20) may be explained by a requirement for a $Mn^{III}_2\text{-Y}\cdot$ cofactor in class Ib RNRs in general.

MATERIALS AND METHODS

Materials

Chemical reagents were obtained from Sigma-Aldrich in the highest purity available unless otherwise indicated. Manganese concentrations were determined using a Perkin Elmer AAnalyst 600 atomic absorption spectrometer. N-terminally His₆-tagged NrdI (HisNrdI) and NrdE² (140 nmol/min/mg, assayed with $Mn^{III}_2\text{-Y}\cdot$ NrdF containing 0.25 Y•/β₂) were purified as reported (21). *E. coli* NrdA (2500–3000 nmol/min/mg), thioredoxin (TR, 40 units/mg), and thioredoxin reductase (TRR, 1400 units/mg) were isolated as described (22–24). NrdA was pre-reduced with DTT, treated with hydroxyurea to reduce any Y• in copurifying endogenous NrdB, and exchanged into assay buffer (50 mM HEPES, 15 mM MgSO₄, 1 mM EDTA, pH 7.6), following the reported procedure (25). Concentrations of NrdA, NrdE, and NrdF are expressed per dimer, and of HisNrdI per monomer. Concentrations of proteins prior to FPLC were assessed by Bradford assay using bovine serum albumin as a standard. After FPLC purification, an ε₂₈₀ of 132 mM⁻¹ cm⁻¹ for NrdF was used. Polyclonal rabbit antibodies to NrdB, NrdF, and NrdI were produced by Covance Research Products. In order to purify antibodies against NrdF, a cell lysate of *E. coli* JW2651 (Table 1) was precipitated with acetone and the antibodies were incubated with a powder produced from drying the precipitate (26). *E. coli* strains GR536 and GR538 were gifts of C. Rensing (U. Arizona) and JW2649 and JW2651 were purchased from the Keio Collection (27,28) (Table 1).

Growth of *E. coli* GR536

E. coli GR536 was grown as previously described (18). A 5 mL culture of LB containing 30 μg/mL kanamycin and 20 μg/mL chloramphenicol was inoculated from a single colony on an LB-agar plate containing the same antibiotics and was grown for ~12 h at 37 °C to an OD₆₀₀ of 2–3. An aliquot (500 μL) was removed, centrifuged at 10000 g for 1 min, resuspended in an equal volume of sterile phosphate-buffered saline (PBS), and used to inoculate 100 mL M9-based minimal medium without antibiotics in a 500 mL baffle flask to an OD₆₀₀ of 0.004. From this point on, no antibiotics were added to the culture media. The minimal medium consisted of 1× M9 salts (11.28 g/L), 0.3% (w/v) Bacto casamino acids (BD), 0.2% (w/v) glycerol, 0.1% (w/v) NaCl, 0.1 mM CaCl₂, and 1 mM MgSO₄. The culture was grown for 10 h at 37 °C with shaking at 220 rpm (final OD₆₀₀ ~ 2). To further decrease cellular iron levels, this culture was diluted 500-fold into another 100 mL minimal medium in a 500 mL baffle flask, which was grown for 2 h at 37 °C with shaking at 220 rpm (final OD₆₀₀ ~ 0.02). This culture was diluted 500-fold into the final, large-scale cultures, which were grown at 37 °C in supplemented minimal medium containing 50 μM 2,2'-dipyridyl and 100 μM MnCl₂ in either a New Brunswick Bioflo 110 fermentor (10 L culture

²The NrdE used in these experiments was purified using PMSF as a protease inhibitor. We have subsequently found that use of PMSF results in ~50% lower specific activity of the purified NrdE than use of Roche Complete protease inhibitor tablets (280 nmol/min/mg).

volume) with 300 rpm stirring and 2.5 L/min aeration, or in 2.8 L baffled flasks (1 L culture volume) or 6 L flasks (2 L culture volume) with shaking at 220 rpm.

Cells were harvested while still in exponential growth at an OD₆₀₀ of 0.5 – 0.7 (13.5–14.5 h in the fermentor or 14.5–17 h in the shaker; doubling times were 50–60 min) by centrifugation at 7000 g for 10 min at 4 °C, flash frozen in liquid N₂, and stored at –80 °C. The OD₆₀₀ of a 100 mL culture grown in parallel containing 2,2'-dipyridyl but without added MnCl₂ was zero after 16 h growth, verifying the reported dependence of this strain on added Mn^{II} for growth (18). Cells were grown in six batches, each starting from a different *E. coli* GR536 colony. From a total culture volume of 91 L, 88 g wet cell paste was obtained.

Purification of NrdF from *E. coli* GR536

In order to minimize the amount of time NrdF was present in the crude cell extract, the first steps in the purification of NrdF from *E. coli* GR536 were carried out in three batches of approximately 30 g wet cell paste. All operations were performed at 4 °C. For each batch, the cell paste was resuspended in 5 mL/g 50 mM Tris, 5% glycerol, pH 7.6 (Buffer A) containing 1 mM phenylmethanesulfonyl fluoride (PMSF), and cells were lysed by passage once through a French pressure cell at 14000 psi. The lysate was centrifuged at 45000 g for 20 min. Ammonium sulfate was added to 60% saturation (390 g/L) over 15 min to the stirred supernatant, followed by 20 min further stirring, and the suspension was centrifuged at 40000 g for 20 min. The pellet was redissolved in ~12 mL of 50 mM sodium phosphate, 5% glycerol, pH 7.0 (Buffer B), containing 1 mM PMSF, and passed through a Sephadex G25 column (2.5 × 35 cm, 170 mL) equilibrated in the same buffer. Protein-containing fractions were identified by their yellow-brown color and pooled (~55–100 mL). HisNrdI (8.5 mg) and DNase (NEB, final concentration 5 U/mL) were added to the pooled fractions and the solution was stirred for 1 h. An equal volume of Buffer B containing 1 M NaCl was added and the protein was loaded onto a Ni-NTA agarose column (1.1 – 2.2 cm, 2 mL) equilibrated with Buffer A containing 500 mM NaCl (Buffer C). The column was washed with 20 CV of Buffer C. The column was then washed with 5 CV Buffer C containing 50 mM imidazole and eluted with 10 CV Buffer C containing 250 mM imidazole. The eluted protein was diluted with Buffer C to ~40 mM imidazole and concentrated to ~40 mL using an Amicon Ultra YM30 centrifugal concentrator (Millipore). The protein solution was flash frozen in liquid nitrogen and stored at –80 °C until further purification. These steps were complete 11–13 h after thawing each batch of cell paste.

The protein solutions from the three preparations (120 mL) were thawed on ice, pooled, and diluted 10-fold in 20 mM HEPES, 5% glycerol, pH 7.0 (Buffer D) containing 10 mM NaCl and concentrated using a Millipore YM30 membrane in an Amicon concentrator to ~500 mL (4 h). The protein solution was loaded onto a DEAE Sepharose Fast Flow column (2.5 × 3 cm, 15 mL) preequilibrated with Buffer D containing 10 mM NaCl. The column was washed with 30 mL Buffer D containing 200 mM NaCl, which was collected in two 15 mL fractions. The protein was then eluted with a 120 mL linear gradient from 200 mM to 1 M NaCl in Buffer D, and 1.7 mL fractions were collected. NrdF-containing fractions were determined by dot blotting with antibodies to NrdF as described below. NrdF eluted in the second wash fraction and elution fractions 1–32. Because a large amount of NrdI was also present in the wash, only the elution fractions 1–32 were pooled (~55 mL, 200–600 mM NaCl). These were concentrated to ~16 mg/mL (450 µL) using an Amicon Ultra YM10 centrifugal concentrator, frozen in liquid N₂, and stored at –80 °C until further purification. These steps were complete 15 h after thawing of the protein solution following Ni-NTA chromatography. The protein was then chromatographed twice using a Poros HQ/20 FPLC anion exchange column (Applied Biosystems, 1.6 × 10 cm, 20 mL, flow rate of 2 mL/min). In the first run, the column was equilibrated with Buffer D containing 200 mM NaCl before

sample loading, and the column was washed with 2 CV Buffer D containing 200 mM NaCl and eluted with a 120 mL linear gradient from 200 to 900 mM NaCl in the same buffer. One-minute fractions (2 mL) were collected. NrdF-containing fractions were identified by SDS-PAGE and dot blotting, and fractions eluting between 35 and 43 min (610–690 mM NaCl) were pooled and concentrated to 320 μ L using Amicon Ultra and Microcon YM10 centrifugal concentrators, frozen in liquid N₂, and stored at -80° C for further purification. The second FPLC step was performed analogously, but the column was equilibrated in Buffer D containing 400 mM NaCl and washed with 1 CV of the same buffer, and the protein was eluted with a 120 mL gradient from 400 to 800 mM NaCl in Buffer D. The NrdF-containing fractions (eluting at \sim 530 mM NaCl) were pooled, concentrated as before, frozen in liquid N₂, and stored at -80° C for analysis. This protocol resulted in NrdF purified to 95% homogeneity.

Detection of NrdF-containing fractions by dot blotting

NrdF-containing fractions after DEAE and FPLC chromatography were determined by spotting 1 or 2 μ L of each fraction onto a 6 \times 10 cm, 0.45 μ m Protran nitrocellulose membrane (Schleicher and Schuell). After drying, the membrane was incubated with gentle shaking at room temperature in 25 mL blocking buffer for 30 min, to which purified antibodies to NrdF were added at 1:10000 dilution and further incubated for 45 min. The membrane was washed three times with 40 mL PBS for 4 min each, incubated with HRP-conjugated goat anti-rabbit secondary antibodies (Thermo Scientific) at 1:2000 dilution in blocking buffer for 45 min, washed three times with 40 mL PBS for 4 min each, developed using SuperSignal West Femto Maximum Sensitivity chemiluminescence reagents (Thermo Scientific), and imaged using a CCD camera (ChemiDoc XRS, Bio-Rad).

Activity assays of NrdF in crude extract/partially purified NrdF

Assays of NrdF in crude extracts and of protein after ammonium sulfate precipitation and Sephadex G25 steps contained in a final volume of 135 μ L: 2.5 mg/mL extract or partially purified protein, 5 μ M NrdE, 0.3 mM dATP, 20 mM dithiothreitol (DTT), 10 mM NaF, and 0.5 mM [³H]-CDP (ViTrax, 5600–21000 cpm/nmol), in assay buffer at 37 $^{\circ}$ C (21). Assays were initiated by addition of NrdF. Aliquots (30 μ L) were removed at 20 s, 3 min, 6 min, and 9 min and heated at 100 $^{\circ}$ C for 2 min. Each aliquot was incubated with 14 U calf intestine alkaline phosphatase (Roche) and 120 nmol deoxycytidine in 75 mM Tris, 0.15 EDTA, pH 8.5, for 2 h at 37 $^{\circ}$ C, and dC was analyzed by the method of Steeper and Steuart (29).

Activity assays of purified NrdF

Assays of NrdF after the Ni-NTA, DEAE, and FPLC steps were performed as above, except 1.0 μ M NrdE was used, no NaF was present, and the concentration of protein in the assay mixture was either 0.5 mg/mL (after Ni-NTA), 0.1 mg/mL (after DEAE), or 0.015 mg/mL (0.2 μ M) NrdF (after FPLC).

Activity assays of NrdB in crude extracts

Assays of NrdB in crude extracts contained in a final volume of 135 μ L: 2.5 mg/mL protein, 5 μ M NrdA, 3 mM ATP, 30 μ M TR, 0.5 μ M TRR, 1 mM NADPH, 10 mM NaF, and 1 mM [³H]-CDP (21000 cpm/nmol), in assay buffer at 37 $^{\circ}$ C (21). Assays were initiated by addition of the extract. Aliquots (30 μ L) were removed at 20 s, 3 min, 6 min, and 9 min and heated at 100 $^{\circ}$ C for 2 min and the samples were worked up as described above.

Western blot analysis of NrdB, NrdF, and NrdI in *E. coli* GR536

E. coli GR536 cells grown as described above and harvested at OD_{600} ~0.08, 0.16, and 0.55, were resuspended in 5 mL/g Buffer A with 1 mM PMSF, lysed by French pressure cell, and centrifuged at 45000 *g* at 4 °C for 20 min. After determination of the protein concentration of the supernatant by Bradford assay, the supernatant was diluted with 2× Laemmli buffer and boiled for 10 min at 100 °C. Because the presence of additional proteins affected transfer of the NrdF and NrdI standards in western blots, extracts of *E. coli* JW2649 and JW2651 (Table 1) were also prepared. These extracts were prepared by a protocol similar to that used for the *E. coli* GR536 extracts, except that the cells were grown in LB to OD_{600} ~0.8 and resuspended in 1 mL/g Buffer B before lysis.

Quantitation of NrdB, NrdF, and NrdI was carried out by western blot analysis as described (30), with the following modifications in the case of NrdF and NrdI. For NrdF, the standard curve used purified NrdF (4–34 ng) mixed with 40 µg *E. coli* JW2651 extract and loaded onto a Criterion 10% Tris-HCl gel (Bio-Rad). *E. coli* GR536 extracts (40 µg) were loaded in duplicate. The gel was run at 200 V for 40 min at 4°C. The proteins were transferred to a PVDF membrane (Bio-Rad) at 200 mA, 4 °C, for 1 h in 25 mM Tris, 195 mM glycine, 15% (v/v) methanol, and 0.01% (w/v) SDS using a Criterion Blotter system (Bio-Rad). The membrane was then handled as described above for dot blotting, with primary antibodies to NrdF added at 1:10000 dilution. For NrdI, the standard curve used purified HisNrdI (0.5–6 ng) mixed with 100 µg *E. coli* JW2649 extract and loaded onto a Criterion 15% Tris-HCl gel. *E. coli* GR536 extracts (100 µg) were loaded in duplicate. The gel was run at 200 V for 45 min at 4°C. The proteins were transferred to a PVDF membrane as above but at 100 V, 4°C, for 80 min. Primary antibodies to NrdI were added at 1:500 dilution.

EPR spectroscopy

EPR spectra of NrdF were acquired on a Bruker EMX X-band spectrometer at 77 K or 4.6 K using an Oxford Instruments liquid helium cryostat. Acquisition parameters were as described (7). Spin quantitation was performed by double integration of the signal and comparison with an *Ec* NrdB sample with known $Y\bullet$ content [determined by the dropline method (31) and by EPR spectroscopy by comparison with a $CuSO_4$ standard (32)]. To ensure a flat baseline, quantitations of $Y\bullet$ in NrdF at 77 K were carried out after subtraction of a buffer sample acquired under identical conditions. Analysis was carried out using WinEPR software (Bruker). The microwave power at half-saturation ($P_{1/2}$) and the inhomogeneous broadening (b) of the $Y\bullet$ signal were calculated as described (7).

RESULTS

NrdF is expressed and active in *E. coli* GR536

Rensing and coworkers have created *E. coli* strains in which multiple transport systems involved in iron uptake were deleted in an effort to study metal specificity of particular transporters (18). Deletions were made in the *feo* (ferrous uptake) and *fec* (ferric citrate) loci, as well as in *entC* (involved in enterobactin biosynthesis for Fe^{III} uptake), *zupT* (a broad specificity divalent cation importer), and *mntH* (a Mn^{II} transporter that also can take up Fe^{II}). When the *E. coli* strain GR536 (Table 1), which lacked all five of these systems, was cultured in minimal media in the presence of 50 µM bipy, only addition of Mn^{II} – not Fe^{II} , Mg^{II} , and Zn^{II} – allowed for normal growth.

Given our recent observation that the *E. coli* class Ib RNR can form a Mn^{III}_2 - $Y\bullet$ cofactor, and that the class Ib RNR of *E. coli* is expressed under iron-limited conditions, we hypothesized that the growth defect of *E. coli* GR536 in the absence of Mn^{II} could be the result of manganese deficiency in the class Ib RNR, limiting deoxynucleotide production

and thus also growth. Therefore, we grew *E. coli* GR536 cells as previously described (18), in M9 minimal media in the presence of 50 μM bipy and 100 μM MnCl_2 , and harvested them in early and mid-exponential growth phases ($\text{OD}_{600} = 0.08, 0.16, \text{ and } 0.55$) when demand for deoxynucleotides is expected to be maximal. Levels of NrdF and NrdB were determined by western blot analysis. Both proteins are expressed under these conditions (Figure 1, Table 2). In mid-exponential phase, NrdF is present at ~ 400 ng/mg total protein and NrdB at ~ 140 ng/mg. The amount of NrdB is comparable to the 190 ng/mg NrdB in *E. coli* K-12 wild type cells grown in LB medium (Yokoyama, Hassan, and Stubbe, unpublished results). Our previous studies had shown that, in vitro, the flavoprotein NrdI is required for $\text{Mn}^{\text{III}}_2\text{-Y}\cdot$ assembly in NrdF (7). Thus, to determine if NrdI is used stoichiometrically or catalytically, western blots were also carried out under the same conditions using antibodies to NrdI. NrdI was determined to be present at $\sim 1/13$ the amount of NrdF (10 ng/mg) and thus probably functions catalytically.

To determine growth conditions that maximized formation of active NrdF, activity assays were carried out on the crude cell extracts at different stages of growth (Table 2). Control experiments showed no cross-reactivity between the class Ia and Ib subunits (see Supporting Information), and therefore both NrdF and NrdB could be assayed in the crude extracts by adding the appropriate $\alpha 2$ subunit (NrdE or NrdA), substrate, and allosteric effector. At $\text{OD}_{600} = 0.55$, the specific activity of NrdF was 0.6 nmol/min/mg total protein (2000 nmol/min/mg NrdF). NrdB protein levels are 3-fold less than NrdF and NrdB activity is ~ 10 -fold less, 0.05 nmol/min/mg total protein (400 nmol/min/mg NrdB). It should be noted that the assays for NrdB activity were carried out with a physiological reducing system (thioredoxin/thioredoxin reductase) while those for NrdF used DTT. These results thus likely underestimate the difference in specific activities of NrdF and NrdB in the crude extracts. Therefore, under these iron-limited growth conditions, the class Ib RNR is the primary source of deoxynucleotides for the cell. The specific activity of NrdF was constant (~ 2200 nmol/min/mg) over the cell densities examined, indicating that the highest yield of active NrdF per liter of culture would be obtained by harvesting cells at $\text{OD}_{600} \sim 0.5$. Thus these growth conditions were chosen as a starting point for purification of NrdF.

Purification of NrdF from *E. coli* GR536

E. coli GR536 harvested at $\text{OD}_{600} = 0.5\text{--}0.7$ gave 88 g wet cell paste from 91 L culture. A summary of the purification of NrdF is shown in Table 3. The central feature of the purification protocol was the addition of His₆-tagged NrdI, known to interact tightly with NrdF (7). Ni-NTA affinity chromatography resulted in 12-fold purification of NrdF. Although a large excess of NrdI was added to the extract to pull out NrdF, only 50% of the NrdF activity was recovered after this step. This is likely due to the extensive washing of the Ni-NTA column carried out to remove the majority of the cellular proteins. The recovery following DEAE anion exchange chromatography was also low; 2/3 of the remaining NrdF activity was lost in the flowthrough and wash of this column. NrdI and NrdF are difficult to separate and, in our experience, the NrdI-NrdF complex does not bind well to anion exchange columns, which probably accounts for the low recovery in this step. It is also possible that the NrdF bound to NrdI has different levels of Mn and Y \cdot than that which is free and thus binds more tightly to the column (see Discussion), but the former fraction was not characterized further. Still, these steps together accomplished 74-fold purification of NrdF. NrdF was further purified by two additional chromatographic steps using a Poros HQ/20 FPLC column (Supporting Information Figures S1 and S2), yielding protein of 95% homogeneity (Figure 2).

NrdF as isolated contains a Mn^{III}₂-Y• cofactor

The UV-visible spectrum of NrdF isolated from *E. coli* GR536 (Figure 3) contains the characteristic sharp and broad features at 408 and 390 nm, respectively, of a Y•. The absence of shoulders at ~325 and 370 nm indicates that the protein has not copurified with a diferric cluster, and the broad absorption feature at ~500 nm is suggestive of a dimanganese(III) cluster (7,33). The purified NrdF contained only 0.86 ± 0.03 Mn/ β 2, assayed by atomic absorption spectroscopy, and thus is mainly in the apo form.

Additional evidence for the presence of a Mn^{III}₂-Y• cofactor in the isolated protein was provided by EPR spectroscopy. We have previously demonstrated that this method allows facile discrimination between the Mn^{III}₂-Y• and Fe^{III}₂-Y• cofactors in NrdF due to differences in their temperature dependence, linewidths, and saturation behavior (7). The EPR spectra of NrdF at 77 and 4.6 K are shown in Figure 4. The Y• signal is identical to that of the Mn^{III}₂-Y• cofactor reconstituted in vitro (7), with strong temperature dependence and linewidths of 450 G at 4.6 K and 130 G at 77 K. The electronic spin relaxation properties ($P_{1/2} = 4.2 \pm 0.6$ mW at 4.6 K, while at 77 K and 100 mW power the signal is only 20% saturated) are also similar to those previously reported for the Mn^{III}₂-Y• cofactor. These properties differ from those of the Fe^{III}₂-Y• signal, which displays little temperature dependence from 3.6 to 293 K, a linewidth of 60 G, and slower electronic spin relaxation ($P_{1/2} = 0.03 \pm 0.01$ mW at 3.6 K). Spin quantitation of the purified NrdF Y• gives 0.20 Y•/ β 2. The specific activity of 720 nmol/min/mg compares well with that observed for Mn^{III}₂-Y• NrdF assembled in vitro with NrdI and O₂ (550 nmol/min/mg for 0.2 Y•/ β 2). By contrast, the specific activity of Fe^{III}₂-Y• NrdF with 0.2 Y•/ β 2 is ~150 nmol/min/mg. Together, the data demonstrate that the active cofactor of NrdF in vivo is a Mn^{III}₂-Y• cofactor identical to that which we recently assembled in vitro.

DISCUSSION

In vivo formation of a dimanganese(III)-Y• cofactor in NrdF

A dimanganese-Y• cofactor was first proposed in 1988 upon isolation of the *C. ammoniagenes* class Ib RNR (14). Over the past two decades, substantial effort has been devoted to establishing that an active manganese cofactor is present in the class Ib RNRs. The class Ib RNRs are structurally homologous to the iron-dependent class Ia enzymes, and when *C. ammoniagenes* and other NrdFs were expressed recombinantly in *E. coli*, iron was incorporated and the protein was active, leading to the misconception that Fe is part of the active metal cofactor inside the cell (8,34). Efforts to isolate NrdFs from *C. ammoniagenes* and *Corynebacterium glutamicum* were successful, but the active cofactors could not be characterized (14,15). Only recently have active class Ib RNRs containing a dimanganese cofactor been successfully obtained and characterized: by cluster assembly in vitro in *E. coli* NrdF, requiring NrdI and O₂ (7), and by overexpression of *C. ammoniagenes* NrdF in its native organism (10).

Thus our efforts to isolate the class Ib RNR from *E. coli* initially focused on conditions to maximize the amount of active enzyme produced. Transcriptional profiling studies under iron limitation and oxidative stress demonstrated elevated levels of mRNA for the class Ib system under these conditions (2–5). In line with earlier studies of mRNA levels (35), preliminary western blots also showed that the level of NrdF was elevated by addition of hydroxyurea, a small molecule known to reduce the Y• in class Ia and Ib RNRs, to the culture medium. After many variations of growth conditions were examined, a strain created by the Rensing group lacking all known iron uptake systems and requiring Mn^{II} for growth in Fe-limited conditions was chosen. Interestingly, growth of a different strain (*E. coli* GR538, see Table 1) containing the Mn^{II} transporter, MntH, in the presence of Mn^{II} led to

no increase in the amount of RNR activity observed in crude extracts relative to *E. coli* GR536 grown under the same conditions (data not shown).

Purification of NrdF was facilitated by taking advantage of our previous observation that NrdI binds tightly to NrdF (7). While this affinity purification was successful, the Mn and Y• contents of the purified protein were substoichiometric. In retrospect, the majority (approximately 2/3) of the activity remaining after the affinity step was lost in the DEAE chromatography step, probably due in large part to the difficulty of separating NrdI from NrdF. Given that NrdI is present at catalytic levels inside the cell, it is likely that the affinity between these two proteins is dependent on the Mn loading of NrdF and the oxidation state of the flavin cofactor of NrdI. It is therefore possible that the NrdF in the discarded fraction may have had higher Mn loading. Efforts to further understand the interactions between these two proteins are in progress.

Low Mn and Y• contents have also been observed in the recent isolation of *C. ammoniagenes* NrdF, in which the level of NrdF expression was genetically manipulated to be 5% of the total protein (10), and in *B. subtilis*, in which NrdF expression was upregulated 20-fold relative to the wild-type levels (Y. Zhang and J. Stubbe, unpublished results). Thus, in the cases examined so far, the growth conditions have been manipulated to maximize amounts of NrdF produced. The substoichiometric amounts of Mn and Y• in these preparations underscores the need to understand the factors involved in NrdF cluster assembly, including regulation of cellular Mn^{II} uptake, the mechanism of Mn^{II} loading of NrdF, and the importance of the levels of NrdF and accessory proteins like NrdI for efficient cofactor assembly.

A number of arguments suggest not only that *E. coli* NrdF can assemble a Mn^{III}₂-Y• cofactor in vivo, but also that it is an obligate manganese protein. First, there is a committed biosynthetic pathway involving NrdI that provides the essential oxidant for cluster formation. Second, if *E. coli* substitutes or supplements its Fe-dependent class Ia RNR with the class Ib RNR in Fe-limited conditions, it is reasonable that the class Ib RNR would not use Fe. A similar situation has been observed in *E. coli* under Fe-limited growth conditions with superoxide dismutase (SOD), in which the Fe-dependent SOD is replaced with a Mn-dependent SOD (36). Third, while it is possible that NrdF is a diiron protein under other growth conditions such as oxidative stress, Imlay and coworkers have pointed out that oxidative stress is simply a special case of Fe limitation. Oxidation of Fe^{II} to Fe^{III}, by H₂O₂ stress, disables the Fe^{II}-responsive transcription factor Fur (37), leading to derepression of Fur-regulated genes such as *nrdHIEF*. Finally, in an elegant set of in vivo experiments, Martin and Imlay have recently provided compelling evidence that manganese is required for function of NrdF inside the cell and that the iron-loaded protein is not sufficiently active to support growth (personal communication). Thus, the independent but complementary approaches in their studies and our own both have led to the conclusion that *E. coli* NrdF is an obligate dimanganese protein.

The role of the class Ib RNR in *E. coli*

The expression of the class Ib RNR in iron limitation and oxidative stress suggests that this system may be especially relevant to *E. coli* and related enterobacteria such as pathogenic *S. Typhimurium* when the bacterium is engulfed by a macrophage, which creates these conditions to weaken and kill invading organisms (38). By extension, the presumptive use of a Mn^{III}₂-Y• cofactor instead of a Fe^{III}₂-Y• may provide insight into why so many other pathogenic organisms depend on class Ib RNRs as their primary aerobic source of deoxynucleotides.

Recent work of Gibert and coworkers has begun to address the role of the class Ib RNR in physiological conditions in *S. Typhimurium* (17). Their studies investigated the survival of $\Delta nrdAB$ and $\Delta nrdEF$ *S. Typhimurium* LT2 strains in a macrophage cell line either possessing or lacking the integral membrane protein Nramp1, which is important in conferring host resistance to infections by pathogens. Phagocytosis of pathogens by macrophages leads to recruitment of Nramp1 to the membrane of the phagosome where it acts as an efflux pump for divalent cations such as Mn^{II} , Fe^{II} , and Zn^{II} from the phagosome (19,39). Gibert and coworkers found that NrdEF appears to play an important role in the early stages of infection, with deletion of *nrdAB* not affecting viability of *S. Typhimurium* in either Nramp1^{+/+} or Nramp1^{-/-} macrophages up to 6 h post-infection. Interestingly, at 24 h, the $\Delta nrdAB$ *S. Typhimurium* was no longer viable in either macrophage cell line, but was still viable at 24 h when infecting Nramp1^{-/-} macrophages in the presence of the Fe^{II} chelator, bipy. One interpretation of these results in light of our own is that, as long as Fe is limiting, NrdEF activity is sufficient to sustain viability of *S. Typhimurium*. The inviability at 24 h in the absence of bipy may be due to the phagosome no longer being sufficiently Fe-limited or oxidatively stressed for class Ib expression to be high enough to support growth.

In support of this hypothesis, the response of the major locus containing *S. Typhimurium* virulence genes, *Salmonella* pathogenicity island 2 (SPI2), to metal efflux by Nramp1 is relatively slow (40). SPI2 has been implicated in promoting survival and replication of the pathogen within the macrophage in part by interfering with localization of the superoxide-producing NADPH oxidase, a major part of the host's oxidative response, to the phagosomal membrane (41). Furthermore, while Nramp1 is directed to the phagosome within 1 h post-infection (39), transcription of the SPI2 genes is not significantly induced until 6 h (40). In the absence of Nramp1, chelation of Fe by bipy is able to induce transcription of these virulence genes as well (40). Therefore, iron limitation and oxidative stress may be particularly severe in the first 6 h of infection, thus providing a window in which the class Ib RNR would be important, until other cellular processes have been mobilized to counteract the macrophage-mounted defense and Fe^{II} becomes more available for metallation of the class Ia RNR (40). Studies of the time-dependence of metal availability in phagosomes would provide further insight into the struggle between host and pathogen for metals. These results must be interpreted with caution, however, as the results of studies in macrophage cell lines can be highly dependent on the host cell type and the specific *S. Typhimurium* strain used (19).

In addition to active NrdEF, *E. coli* GR536 cells also contain substantial amounts of largely inactive NrdAB; this may not be so surprising, however, as unlike *nrdHIEF*, there is no evidence that *nrdAB* is regulated by cellular iron levels via Fur. NrdB could be predominantly in the apo form or, given that Mn^{II} binds more tightly to NrdB than Fe^{II} (42), loaded with Mn^{II} , which cannot be converted to active cofactor³. The presence of a large amount of NrdAB with low activity may suggest that such extreme Fe limitation is not likely to be physiologically relevant for *E. coli* and that the role of the class Ib RNR is to supplement, rather than completely replace, class Ia function in iron limitation and oxidative stress. Alternatively, inactive NrdB (Mn^{II} -loaded or apo) may remain in expectation of the higher iron levels that would allow its activation. Further studies are required to elucidate the factors controlling NrdAB and NrdEF expression levels and activity in *E. coli*.

Are all NrdFs dimanganese proteins? a. The role of NrdI

The question of whether all NrdFs, like those of *E. coli* and *C. ammoniagenes*, use manganese or if some use iron must be addressed on an organism-by-organism basis.

³In vitro incubation of Mn^{II}_2 -NrdB with reduced NrdI and O_2 fails to generate $Y\bullet$ and activity (see Supporting Information).

Growth and expression conditions, differences in metal homeostatic mechanisms, cellular metal concentrations, and relative binding affinities of different NrdFs for Mn^{II} and Fe^{II} all are important factors. The paucity of this information for most organisms utilizing class Ib RNRs makes evaluation of this issue difficult. However, the requirement of NrdI for assembly of the Mn^{III}₂-Y• cofactor (7), and biochemical (21) and structural (9,43,44) characterization of NrdI, allows us to begin to address this question indirectly.

We have proposed that NrdI's role in Mn^{III}₂-Y• assembly is to reduce O₂ by two electrons to HOO(H) (7). This reaction is governed by the redox potentials of its flavin cofactor. The factors responsible for modulation of these potentials have been studied extensively. Based on these studies, we have previously suggested that NrdI's ability to reduce O₂ to HOO(H) (7) arises from two factors: the positive electrostatic environment of the flavin and the presence of a flexible loop region ("50s loop") near the flavin N5 and reactive C4a positions, able to hydrogen bond with the flavin in both the oxidized and fully reduced states. These hypotheses are strongly supported by the x-ray structures of these forms of NrdI in complex with NrdF (9).

As previously observed for NrdFs (45), genomic analysis reveals that NrdIs can be grouped into three major classes that correlate with the length and composition of the 50s loop [see (44) for a phylogenetic tree]. The proposed structure-function relationships outlined above, along with the available biochemical and physiological data, suggest that NrdIs of the same phylogenetic group function similarly.

The first and largest subclass of NrdIs includes the proteins from *E. coli* and *C. ammoniagenes*, which both assemble dimanganese(III)-Y• cofactors in vivo. *S. pyogenes* NrdI1 (NrdI*) also falls into this class and has been reported to be essential for activity of its class Ib RNR (46); it is thus also likely to be involved in Mn^{III}₂-Y• cofactor assembly. NrdIs of a second and smaller class have longer 50s loops than the first. One member of this class is *Lactobacillus plantarum*, an organism that accumulates mM levels of Mn, appears not to require Fe for growth (47), and uses a class Ib RNR for aerobic growth. It is therefore reasonable to predict that this class also uses a manganese cofactor.

NrdIs of the third class contain three-residue 50s loops not capable of hydrogen bonding to the flavin in the oxidized state. These NrdIs are found predominantly in *Bacillus* and *Staphylococcus*, including *Bacillus cereus* (43) and *B. anthracis* (44). The function of the NrdIs in this class are less clear, as they stabilize higher amounts of the one-electron reduced semiquinone form of the cofactor than *E. coli* NrdI (~60% for *B. anthracis*, near-stoichiometric for *B. cereus*, compared to 28% for *E. coli*). The increased levels of semiquinone may suggest that the flavins are inefficient two-electron reductants of O₂ (9,44). These NrdIs could be involved in Y• maintenance (30) or provide the extra electron required for assembly of a diferric-Y• cofactor. However, their redox properties could easily be modulated by interaction with NrdF to favor reduction of O₂ to HOO(H), as the presence of NrdF clearly perturbs the electrostatic environment of the flavin cofactor of the *E. coli* NrdI (7,9). Alternatively, assembly of a Mn^{III}₂-Y• cofactor by a different mechanism in these NrdFs (for example, with NrdI providing a different oxidant, superoxide) cannot be ruled out. No experiments on the feasibility of Mn^{III}₂-Y• cluster assembly in *B. anthracis* or *B. cereus* NrdFs have been reported. Interestingly, however, experiments from our laboratory (Y. Zhang and J. Stubbe, unpublished results) have shown that NrdF from the closely related *B. subtilis* assembles a Mn^{III}₂-Y• cofactor in vivo. We therefore propose that the Mn^{III}₂-Y• cofactor demonstrated in *E. coli* will also be found in the class Ib RNRs of all three phylogenetic groups.

b. The essential physiological role of Mn

A large number of prokaryotes have been documented to require Mn for growth and, in the case of pathogens, virulence. Some, like *Lactobacillus plantarum* (47) and the radiation-resistant *Deinococcus radiodurans* (48), which both encode class Ib RNRs, do not require iron for aerobic growth and accumulate high levels of intracellular Mn, as determined by metal analysis of cell extracts. While other prokaryotes that depend on class Ib RNRs for aerobic growth have not completely done away with a requirement for iron, they also have been shown to accumulate high levels of Mn. The affinities of regulators of Mn^{II} transport, for example MntR from *B. subtilis* and AntR from *B. anthracis* AntR, are high – 60 and 160 μ M, respectively (49,50) – suggesting that the concentration range of weakly bound Mn^{II} in these organisms may be of a similar order. Mn^{II} has also been reported to be crucial for full virulence of the pathogenic organisms including *S. Typhimurium*, *S. aureus*, and *S. pyogenes* (19,39,51). In fact, the host's immune response devotes much energy to making both Fe^{II} and Mn^{II} limiting nutrients in the phagosome.

Despite the importance of manganese, the essential roles that it plays are not well understood. Relatively few enzymes have an absolute requirement for this metal. A longstanding hypothesis is that one of the major physiological functions of the high levels of Mn^{II}, complexed mostly with phosphates and nucleotides in the cell, is to counteract oxidative stress by acting as a superoxide dismutase (SOD) to disproportionate superoxide into H₂O₂ and O₂ (47). This proposal is supported by in vitro studies of Mn^{II}-phosphate complexes (52) and recently by electron nuclear double resonance spectroscopic studies of whole *S. cerevisiae* cells (53). Such a role could be particularly important for pathogens, as superoxide is a key part of the host's oxidative defense. Alternatively, the essential role of Mn^{II} may be related to MnSOD activity. Others have suggested that Mn^{II} can act as an essential Lewis acid in some enzymes (13,19), especially to replace Fe^{II} in certain conditions to prevent oxidative damage by Fenton chemistry (13).

Fe and Mn homeostasis appears to be quite different in the bacteria described above than in *E. coli*, which may explain why *E. coli* and related enterobacteriaceae are the only prokaryotes that contain both class Ia and Ib RNRs, and why their class Ib RNRs are expressed only during iron limitation and oxidative stress. Overexpression of all NrdFs reported to date in *E. coli* grown in rich medium leads to incorporation of Fe and diferric-Y• formation with widely varying levels. By contrast, when *C. ammoniagenes* NrdF is overexpressed in its native organism in the presence of iron, it is still not loaded with iron (10). In *E. coli* grown in a defined minimal medium, Mn levels are quite low – ~15 μ M (13) – compared with ~1 mM Fe (54), although most of this Fe is not readily bioavailable (55). No Mn^{II} chaperones are known, and we suggest that bioavailable iron levels are normally too high and manganese levels too low in enterobacteriaceae to metallate the class Ib RNR correctly with manganese, and only in Fe limitation or oxidative stress is the ratio of free Mn^{II} to Fe^{II} high enough to allow Mn^{II} to effectively compete with Fe^{II} for binding to NrdF. In other class Ib-containing organisms, metal homeostasis may be controlled in such a way that there is less Fe^{II} and more bioavailable Mn^{II} for loading NrdF, such that it is correctly metallated with Mn^{II} in normal growth.

We propose that the Mn requirement of many prokaryotes is linked, at least in part, to a Mn requirement for the class Ib RNR. The essential function of RNR for deoxynucleotide provision for replication and DNA repair is an obvious explanation for a requirement for Mn. The Mn-dependence, rather than Fe-dependence, of the class Ib RNRs of these organisms may reflect the struggle between host and pathogen for essential metals.

Conclusion

The activity of *E. coli* (7) and *C. ammoniagenes* (10) NrdFs with both Fe^{III}₂-Y• and Mn^{III}₂-Y• cofactors demonstrates that the metal coordination environment in NrdF itself is not the primary determinant of the NrdF's active form. Instead, the redox properties of NrdI, the mechanism of metallation of NrdF, cellular Mn and Fe homeostasis, and regulation of RNR expression all appear to play roles. The biochemical and physiological data presented here argue that most, if not all, class Ib RNRs are dimanganese proteins *in vivo*. Ultimately, however, parallel *in vitro* and *in vivo* studies of a number of class Ib RNR systems, such as we have presented here and in our previous work (7,21), will be necessary to determine 1) whether all class Ib RNRs contain dimanganese(III)-Y• cofactors inside the cell, and 2) what factors are responsible for imparting cofactor specificity *in vivo*.

Supplementary Material

Refer to Web version on PubMed Central for supplementary material.

Acknowledgments

We thank J. A. Imlay for thoughtful comments on a previous version of this manuscript and we thank him and J. Martin for sharing a draft of their manuscript prior to its submission. We are grateful to S. J. Lippard for use of his laboratory's atomic absorption spectrometer and J. Wilson for assistance in data acquisition, B. Imperiali for use of her laboratory's fermentor, and C. Rensing for the generous gift of *E. coli* GR536 and GR538. We also thank E. C. Minnihan, K. Yokoyama, and Y. Aye for preparing the NrdA, TR, and TRR used in these studies.

References

1. Nordlund P, Reichard P. Ribonucleotide reductases. *Annu Rev Biochem.* 2006; 75:681–706. [PubMed: 16756507]
2. McHugh JP, Rodriguez-Quinones F, Abdul-Tehrani H, Svistunenko DA, Poole RK, Cooper CE, Andrews SC. Global iron-dependent gene regulation in *Escherichia coli*. A new mechanism for iron homeostasis. *J Biol Chem.* 2003; 278:29478–29486. [PubMed: 12746439]
3. Vassinova N, Kozzyrev D. A method for direct cloning of Fur-regulated genes: identification of seven new Fur-regulated loci in *Escherichia coli*. *Microbiology.* 2000; 146:3171–3182. [PubMed: 11101675]
4. Monje-Casas F, Jurado J, Prieto-Alamo MJ, Holmgren A, Pueyo C. Expression analysis of the *nrdHIEF* operon from *Escherichia coli*. Conditions that trigger the transcript level *in vivo*. *J Biol Chem.* 2001; 276:18031–18037. [PubMed: 11278973]
5. Gon S, Faulkner MJ, Beckwith J. *In vivo* requirement for glutaredoxins and thioredoxins in the reduction of the ribonucleotide reductases of *Escherichia coli*. *Antioxid Redox Signal.* 2006; 8:735–742. [PubMed: 16771665]
6. Lundin D, Torrents E, Poole AM, Sjöberg BM. RNRdb, a curated database of the universal enzyme family ribonucleotide reductase, reveals a high level of misannotation in sequences deposited to Genbank. *BMC Genomics.* 2009; 10:589–596. [PubMed: 19995434]
7. Cotruvo JA Jr, Stubbe J. An active dimanganese(III)-tyrosyl radical cofactor in *Escherichia coli* class Ib ribonucleotide reductase. *Biochemistry.* 2010; 49:1297–1309. [PubMed: 20070127]
8. Jordan A, Pontis E, Atta M, Krook M, Gibert I, Barbé J, Reichard P. A second class I ribonucleotide reductase in *Enterobacteriaceae*: Characterization of the *Salmonella typhimurium* enzyme. *Proc Natl Acad Sci USA.* 1994; 91:12892–12896. [PubMed: 7809142]
9. Boal AK, Cotruvo JA Jr, Stubbe J, Rosenzweig AC. Structural basis for activation of class Ib ribonucleotide reductase. *Science.* 2010; 329:1526–1530. [PubMed: 20688982]
10. Cox N, Ogata H, Stolle P, Reijerse E, Auling G, Lubitz W. A tyrosyl-dimanganese coupled spin system is the native metalloradical cofactor of the R2F subunit of the ribonucleotide reductase of *Corynebacterium ammoniagenes*. *J Am Chem Soc.* 2010; 132:11197–11213. [PubMed: 20698687]

11. Stolle P, Barckhausen O, Oehlmann W, Knobbe N, Vogt C, Pierik AJ, Schmidt PP, Reijerse EJ, Lubitz W, Auling G. Homologous expression of the *nrdF* gene of *Corynebacterium ammoniagenes* strain ATCC 6872 generates a manganese-metallocofactor (R2F) and a stable tyrosyl radical (Y•) involved in ribonucleotide reduction. *FEBS J.* 2010; 277:4849–4862. [PubMed: 20977673]
12. Naranuntarat A, Jensen LT, Pazicni S, Penner-Hahn JE, Culotta VC. The interaction of mitochondrial iron with manganese superoxide dismutase. *J Biol Chem.* 2009; 284:22633–22640. [PubMed: 19561359]
13. Anjem A, Varghese S, Imlay JA. Manganese import is a key element of the OxyR response to hydrogen peroxide in *Escherichia coli*. *Mol Microbiol.* 2009; 72:844–858. [PubMed: 19400769]
14. Willing A, Follmann H, Auling G. Ribonucleotide reductase of *Brevibacterium ammoniagenes* is a manganese enzyme. *Eur J Biochem.* 1988; 170:603–611. [PubMed: 2828045]
15. Fieschi F, Torrents E, Touloukhouva L, Jordan A, Hellman U, Barbe J, Gibert I, Karlsson M, Sjöberg BM. The manganese-containing ribonucleotide reductase of *Corynebacterium ammoniagenes* is a class Ib enzyme. *J Biol Chem.* 1998; 273:4329–4337. [PubMed: 9468481]
16. Abbouni B, Oehlmann W, Stolle P, Pierik AJ, Auling G. Electron paramagnetic resonance (EPR) spectroscopy of the stable-free radical in the native metallo-cofactor of the manganese-ribonucleotide reductase (Mn-RNR) of *Corynebacterium glutamicum*. *Free Radic Res.* 2009; 43:943–950. [PubMed: 19707921]
17. Panosa A, Roca I, Gibert I. Ribonucleotide reductases of *Salmonella* Typhimurium: Transcriptional regulation and differential role in pathogenesis. *PLoS ONE.* 2010; 5:e11328. [PubMed: 20593029]
18. Grass G, Franke S, Taudte N, Nies DH, Kucharski LM, Maguire ME, Rensing C. The metal permease ZupT from *Escherichia coli* is a transporter with a broad substrate spectrum. *J Bacteriol.* 2005; 187:1604–1611. [PubMed: 15716430]
19. Papp-Wallace KM, Maguire ME. Manganese transport and the role of manganese in virulence. *Annu Rev Microbiol.* 2006; 60:187–209. [PubMed: 16704341]
20. Kehl-Fie TE, Skaar EP. Nutritional immunity beyond iron: a role for manganese and zinc. *Curr Opin Chem Biol.* 2010; 14:218–224. [PubMed: 20015678]
21. Cotruvo JA Jr, Stubbe J. NrdI, a flavodoxin involved in maintenance of the diferric-tyrosyl radical cofactor in *Escherichia coli* class Ib ribonucleotide reductase. *Proc Natl Acad Sci USA.* 2008; 105:14383–14388. [PubMed: 18799738]
22. Yee CS, Seyedsayamdost MR, Chang MCY, Nocera DG, Stubbe J. Generation of the R2 subunit of ribonucleotide reductase by intein chemistry: Insertion of 3-nitrotyrosine at residue 356 as a probe of the radical initiation process. *Biochemistry.* 2003; 42:14541–14552. [PubMed: 14661967]
23. Chivers PT, Prehoda KE, Volkman BF, Kim B-M, Markley JL, Raines RT. Microscopic pK_a values of *Escherichia coli* thioredoxin. *Biochemistry.* 1997; 36:14985–14991. [PubMed: 9398223]
24. Russel M, Model P. Direct cloning of the *trxB* gene that encodes thioredoxin reductase. *J Bacteriol.* 1985; 163:238–242. [PubMed: 2989245]
25. Seyedsayamdost MR, Xie J, Chan CTY, Schultz PG, Stubbe J. Site-specific insertion of 3-aminotyrosine into the $\alpha 2$ subunit of *E. coli* ribonucleotide reductase: Direct evidence for involvement of Y730 and Y731 in radical propagation. *J Am Chem Soc.* 2007; 129:15060–15071. [PubMed: 17990884]
26. Harlow, E.; Lane, D. *Antibodies: A laboratory manual.* Cold Spring Harbor Laboratory; Cold Spring: 1988.
27. Baba T, Ara T, Hasegawa M, Takai Y, Okumura Y, Baba M, Datsenko KA, Tomita M, Wanner BL, Mori H. Construction of *Escherichia coli* K-12 in-frame, single-gene knock-out mutants - the Keio collection. *Mol Systems Biol.* 2006; 2:2006.0008.
28. Datsenko K, Wanner BL. One-step inactivation of chromosomal genes in *Escherichia coli* K-12 using PCR products. *Proc Natl Acad Sci U S A.* 2000; 97:6640–6645. [PubMed: 10829079]
29. Steeper JR, Steuart CD. A rapid assay for CDP reductase activity in mammalian cell extracts. *Anal Biochem.* 1970; 34:123–130. [PubMed: 5440901]

30. Hristova D, Wu C-H, Stubbe J. Importance of the maintenance pathway in the regulation of the activity of *Escherichia coli* ribonucleotide reductase. *Biochemistry*. 2008; 47:3989–3999. [PubMed: 18314964]
31. Bollinger JM Jr, Tong WH, Ravi N, Huynh BH, Edmondson DE, Stubbe J. Use of rapid kinetics methods to study the assembly of the diferric-tyrosyl radical cofactor of *Escherichia coli* ribonucleotide reductase. *Methods Enzymol*. 1995; 258:278–303. [PubMed: 8524156]
32. Malmström BG, Reinhammar B, Vanngard T. The state of copper in stellacyanin and laccase from the lacquer tree *Rhus vernicifera*. *Biochim Biophys Acta*. 1970; 205:48–57. [PubMed: 4314765]
33. Whittaker MM, Barynin VV, Antonyuk SV, Whittaker JW. The oxidized (3,3) state of manganese catalase. Comparison of enzymes from *Thermus thermophilus* and *Lactobacillus plantarum*. *Biochemistry*. 1999; 38:9126–9136. [PubMed: 10413487]
34. Huque Y, Fieschi F, Torrents E, Gibert I, Eliasson R, Reichard P, Sahlin M, Sjöberg BM. The active form of the R2F protein of class Ib ribonucleotide reductase from *Corynebacterium ammoniagenes* is a diferric protein. *J Biol Chem*. 2000; 275:25365–25371. [PubMed: 10801858]
35. Jordan A, Aragall E, Gibert I, Barbé J. Promoter identification and expression analysis of *Salmonella typhimurium* and *Escherichia coli* *nrdEF* operons encoding one of two class I ribonucleotide reductases present in both bacteria. *Mol Microbiol*. 1996; 19:777–790. [PubMed: 8820648]
36. Fee JA. Regulation of *sod* genes in *Escherichia coli*: relevance to superoxide dismutase function. *Mol Microbiol*. 1991; 5:2599–2610. [PubMed: 1779751]
37. Varghese S, Wu A, Park S, Imlay KRC, Imlay JA. Submicromolar hydrogen peroxide disrupts the ability of Fur protein to control free-iron levels in *Escherichia coli*. *Mol Microbiol*. 2007; 64:822–830. [PubMed: 17462026]
38. Flannagan RS, Cosio G, Grinstein S. Antimicrobial mechanisms of phagocytes and bacterial evasion strategies. *Nat Rev Microbiol*. 2009; 7:355–366. [PubMed: 19369951]
39. Jabado N, Jankowski A, Dougaparsad S, Picard V, Grinstein S, Gros P. Natural resistance to intracellular infections: Natural resistance-associated macrophage protein 1 (NRAMP1) functions as a pH-dependent manganese transporter at the phagosomal membrane. *J Exp Med*. 2000; 192:1237–1247. [PubMed: 11067873]
40. Zaharik ML, Vallance BA, Puente JL, Gros P, Finlay BB. Host-pathogen interactions: Host resistance factor Nramp1 up-regulates the expression of *Salmonella* pathogenicity island-2 virulence genes. *Proc Natl Acad Sci U S A*. 2002; 99:15705–15710. [PubMed: 12441401]
41. Vazquez-Torres A, Xu Y, Jones-Carson J, Holden DW, Lucia SM, Dinauer MC, Mastroeni P, Fang FC. *Salmonella* pathogenicity island 2-dependent evasion of the phagocyte NADPH oxidase. *Science*. 2000; 287:1655–1658. [PubMed: 10698741]
42. Atta M, Nordlund P, Aberg A, Eklund H, Fontecave M. Substitution of manganese for iron in ribonucleotide reductase from *Escherichia coli*: Spectroscopic and crystallographic characterization. *J Biol Chem*. 1992; 267:20682–20688. [PubMed: 1328209]
43. Røhr ÅK, Hersleth HP, Andersson KK. Tracking flavin conformations in protein crystal structures with Raman spectroscopy and QM/MM calculations. *Angew Chem Int Ed*. 2010; 49:2324–2327.
44. Johansson R, Torrents E, Lundin D, Sprenger J, Sahlin M, Sjöberg BM, Logan DT. High-resolution crystal structures of the flavoprotein NrdI in oxidized and reduced states - an unusual flavodoxin. *FEBS J*. 2010; 277:4265–4277. [PubMed: 20831589]
45. Torrents E, Sahlin M, Biglino D, Gräslund A, Sjöberg BM. Efficient growth inhibition of *Bacillus anthracis* by knocking out the ribonucleotide reductase tyrosyl radical. *Proc Natl Acad Sci USA*. 2005; 102:17946–17951. [PubMed: 16322104]
46. Roca I, Torrents E, Sahlin M, Gibert I, Sjöberg BM. NrdI essentiality for class Ib ribonucleotide reduction in *Streptococcus pyogenes*. *J Bacteriol*. 2008; 190:4849–4858. [PubMed: 18502861]
47. Archibald FS, Fridovich I. Manganese and defenses against oxygen toxicity in *Lactobacillus plantarum*. *J Bacteriol*. 1981; 145:442–451. [PubMed: 6257639]
48. Daly MJ, Gaidamakova EK, Matrosova VY, Vasilenko A, Zhai M, Venkateswaran A, Hess M, Omelchenko MV, Kostandarites HM, Makarova KS, Wackett LP, Fredrickson JK, Ghosal D. Accumulation of Mn(II) in *Deinococcus radiodurans* facilitates gamma-radiation resistance. *Science*. 2004; 306:1025–1028. [PubMed: 15459345]

49. Golynskiy MV, Gunderson WA, Hendrich MP, Cohen SM. Metal binding studies and EPR spectroscopy of the manganese transport regulator MntR. *Biochemistry*. 2006; 45:15359–15372. [PubMed: 17176058]
50. Sen KI, Sienkiewicz A, Love JF, vanderSpek JC, Fajer PG, Logan TM. Mn(II) binding by the anthracis repressor from *Bacillus anthracis*. *Biochemistry*. 2006; 45:4295–4303. [PubMed: 16566604]
51. Corbin BD, Seeley EH, Raab A, Feldmann J, Miller MR, Torres VJ, Anderson KL, Dattilo BM, Dunman PM, Gerads R, Caprioli RM, Nacken W, Chazin WJ, Skaar EP. Metal chelation and inhibition of bacterial growth in tissue abscesses. *Science*. 2008; 319:962–965. [PubMed: 18276893]
52. Barnese K, Gralla EB, Cabelli DE, Valentine JS. Manganous phosphate acts as a superoxide dismutase. *J Am Chem Soc*. 2008; 130:4604–4606. [PubMed: 18341341]
53. McNaughton RL, Reddi AR, Clement MHS, Sharma A, Barnese K, Rosenfeld L, Gralla EB, Valentine JS, Culotta VC, Hoffman BM. Probing in vivo Mn²⁺ speciation and oxidative stress resistance in yeast cells with electron-nuclear double resonance spectroscopy. *Proc Natl Acad Sci U S A*. 2010; 107:15335–15339. [PubMed: 20702768]
54. Outten CE, O'Halloran TV. Femtomolar sensitivity of metalloregulatory proteins controlling zinc homeostasis. *Science*. 2001; 292:2488–2492. [PubMed: 11397910]
55. Keyer K, Imlay JA. Superoxide accelerates DNA damage by elevating free-iron levels. *Proc Natl Acad Sci U S A*. 1996; 93:13635–13640. [PubMed: 8942986]

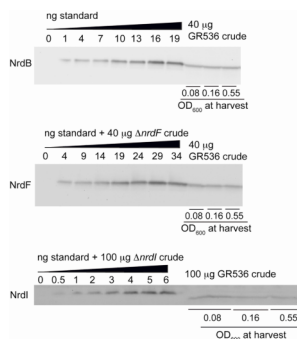


FIGURE 1.

Representative western blots to determine the levels of NrdB, NrdF, and NrdI in *E. coli* GR536 cells harvested at $OD_{600} = 0.08, 0.16, \text{ and } 0.55$. Standards for quantitation are in lanes 1–8. Lanes 9–11 (NrdB and NrdF blots) and 9–14 (NrdI blot) show the amount of each protein in *E. coli* GR536 crude cell extracts. For the NrdF and NrdI standard lanes, crude extracts of $\Delta nrdf$ (40 μg) and $\Delta nrDI$ (100 μg) deletion strains were added. Note that HisNrdI was used as the standard for the NrdI blots, and that these standards run slightly slower (~ 2 kDa) than the untagged NrdI band in the extract. The samples are shown in duplicate for the NrdI blot.

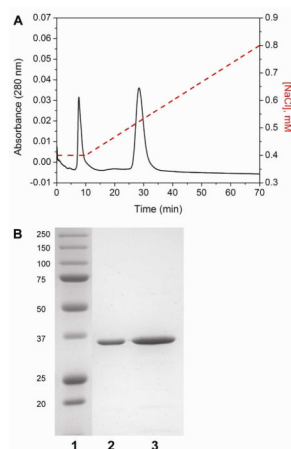


FIGURE 2.

NrdF from *E. coli* GR536 is purified to near homogeneity. A) Elution profile from the second FPLC step. NrdF eluted at 29 min. B) SDS-PAGE (12.5%) analysis. Lane 1: molecular weight standards (kDa). Lanes 2 and 3: NrdF, 1 and 3 μg, respectively.

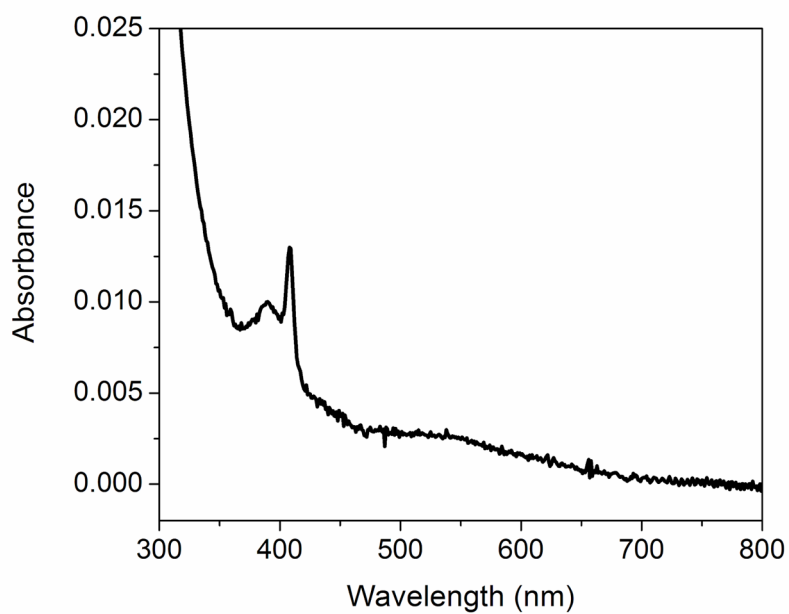


FIGURE 3. Visible spectrum of NrdF (7 μ M) isolated from its endogenous levels in *E. coli* GR536. The spectrum is consistent with that of the dimanganese(III)-Y• cofactor previously described (7).

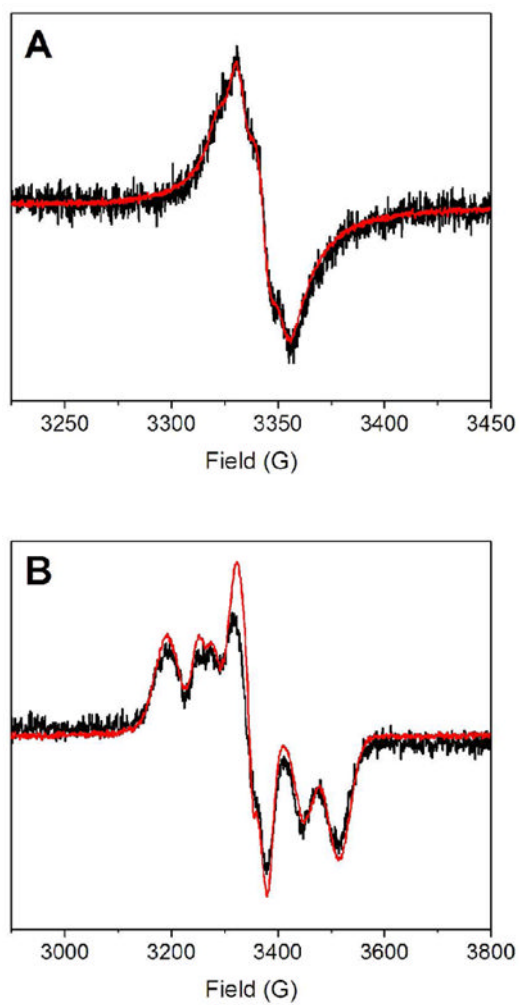


FIGURE 4. EPR spectra of NrdF from *E. coli* GR536 after the first FPLC step (black) overlaid with $\text{Mn}^{\text{III}}_2\text{-Y}\cdot$ reconstituted in vitro (red). A) At 77 K. B) At 4.6 ± 0.2 K.

TABLE 1*E. coli* strains used in this study

Strain	Genotype	Reference
GR536	W3110 $\Delta fecABCDE::kan \Delta zupT::cat \Delta mntH \Delta entC \Delta feoABC$	(18)
GR538	W3110 $\Delta fecABCDE::kan \Delta zupT::cat \Delta entC \Delta feoABC$	(18)
JW2649	BW25113 $\Delta nrdI755::kan$	(27)
JW2651	BW25113 $\Delta nrdF757::kan$	(27)

TABLE 2

Protein levels and specific activities of class Ia and Ib RNRs in crude extracts

OD ₆₀₀	Protein level (ng/mg protein) ^d			Specific activity (nmol/min/mg protein)			Specific activity (nmol/min/mg β ₂) ^d		
	NrdF	NrdB	NrdI	NrdF ^b	NrdB ^c	NrdI	NrdF	NrdB	NrdI
0.08	450 ± 180	160 ± 10	16 ± 3	1.1	0.08 ± 0.02		2400 ± 1000		500 ± 100
0.16	370 ± 90	140 ± 40	10 ± 1	0.8 ± 0.1	0.09 ± 0.03		2200 ± 600		600 ± 300
0.55	300 ± 110	120 ± 50	9 ± 3	0.6 ± 0.1	0.05 ± 0.01		2000 ± 800		400 ± 200

^aDetermined by western blotting^bRadioactive assay, 5 μM NrdE, DTT, 37 °C^cRadioactive assay, 5 μM NrdA, TR, TRR, NADPH, 37 °C^dSpecific activities normalized for the β₂ (NrdF or NrdB) levels determined by western blotting

TABLE 3

Purification of NrdF from *E. coli* GR536^a

Purification step	Protein (mg)	Total activity (nmol/min)	Specific activity (nmol/min/mg)	Percent recovery	Purification factor
Crude extract ^b	7100	5400	0.76	100	1
(NH ₄) ₂ SO ₄ / G25 ^b	5400	2100	0.39	40	0.5
Ni-NTA	140	1200	8.8	22	12
DEAE	7.1	400	56	7	74
FPLC 1	0.39	230	580	4	780
FPLC 2	0.15	110	720	2	950

^aNrdF was purified from 88 g of cells^bThe results shown for these steps represent the aggregate of 3 separate purifications from ~30 g cells